Hindawi
Journal of Chemistry
Volume 2020, Article ID 4809127, 10 pages
https://doi.org/10.1155/2020/4809127

Research Article

Highly Selective Reduction of Bio-Based Furfural to Furfuryl Alcohol Catalyzed by Supported KF with Polymethylhydrosiloxane (PMHS)

Zhaozhuo Yu, Weibo Wu, Hu Li, and Song Yang

State Key Laboratory Breeding Base of Green Pesticide & Agricultural Bioengineering, Key Laboratory of Green Pesticide & Agricultural Bioengineering, Ministry of Education, State-Local Joint Laboratory for Comprehensive Utilization of Biomass, Center for Research & Development of Fine Chemicals, Guizhou University, Guiyang, Guizhou 550025, China

Correspondence should be addressed to Hu Li; hli13@gzu.edu.cn and Song Yang; jhzx.msm@gmail.com

Received 13 August 2019; Revised 26 November 2019; Accepted 11 December 2019; Published 28 January 2020

Academic Editor: Antonio De Lucas-Consuegra

Hydrogenation of bio-based furfural (FUR) to furfuryl alcohol (FFA) is tremendously expanding the application of biomass in many industries such as resins, biofuels, and pharmaceuticals. However, mass manufacture of FFA from FUR is restrained by strict requirements of reaction conditions and expensive catalysts. In this work, an economical and benign catalytic system, containing an easily prepared and reusable catalyst 5 wt.% KF/ZrO_2 and a low-cost hydrogen source polymethylhydrosiloxane (PMHS), was developed to be efficient for the hydrogenation of FUR to high-value FFA under mild conditions. The catalyst reactivity was found to be remarkably influenced by the support acid-base properties and KF loading doge. In the presence of 5 wt.% KF/ZrO_2, a high FFA yield of 97% and FUR conversion of 99% could be obtained at 25°C in just 0.5 h, which was superior to those attained with other tested catalysts. The KF/ZrO_2 catalyst could be recycled at least five times, with the FFA yield slightly decreasing from 97% to 71%. The spare decrease in FFA yield is possibly attributed to the catalyst pore blocking, as clarified by SEM, BET, XPS, and ICP-MS measurements of the fresh and reused catalysts.

1. Introduction

Diversiform sustainable clean energies have been developed to get rid of the dependence of nonrenewable fossil energy and relieve environmental deterioration caused by combustion of fossil fuel in past decades [1–3]. In particular, biomass containing abundant carbon source is considered as the best source to replace fossil fuels, for the production of various biofuels such as biodiesel, ethanol, and 2,5-dimethylfuran [4–8]. In addition, through a series of chemical reactions including hydrolysis, dehydration, oxidation, hydrogenation, and hydrogenolysis, lignocellulosic biomass can be transformed into numerous value-added oxygen-containing heterocyclic compounds [9–17].

Furfural (FUR) is an important biomass-derived compound, which is mainly obtained from the xylose which is one of the main hydrolyzates of hemicellulose [18, 19]. Through the partial reduction of FUR, furfuryl alcohol (FFA) can be prepared. FFA is indispensable feedstock for the synthesis of diverse downstream compounds including ethyl furfuryl ether, tetrahydrofurfuryl alcohol, γ-valerolactone, levulinic acid, and so on, all of which have wide applications in fuels, pharmaceuticals, and food and chemical industries (Figure 1) [20–29]. Up to now, artificial synthesis of FUR and FFA is of high cost and needs a complex conversion process, indicating that the hydrogenation of FUR not only enlarges the application of biomass but also sharply decreases the synthesis cost of various downstream compounds [30, 31].

The H-donor for the hydrogenation of FUR to FFA is classified as gas- and liquid-phase reaction processes, all of which have corresponding advantages and shortages.

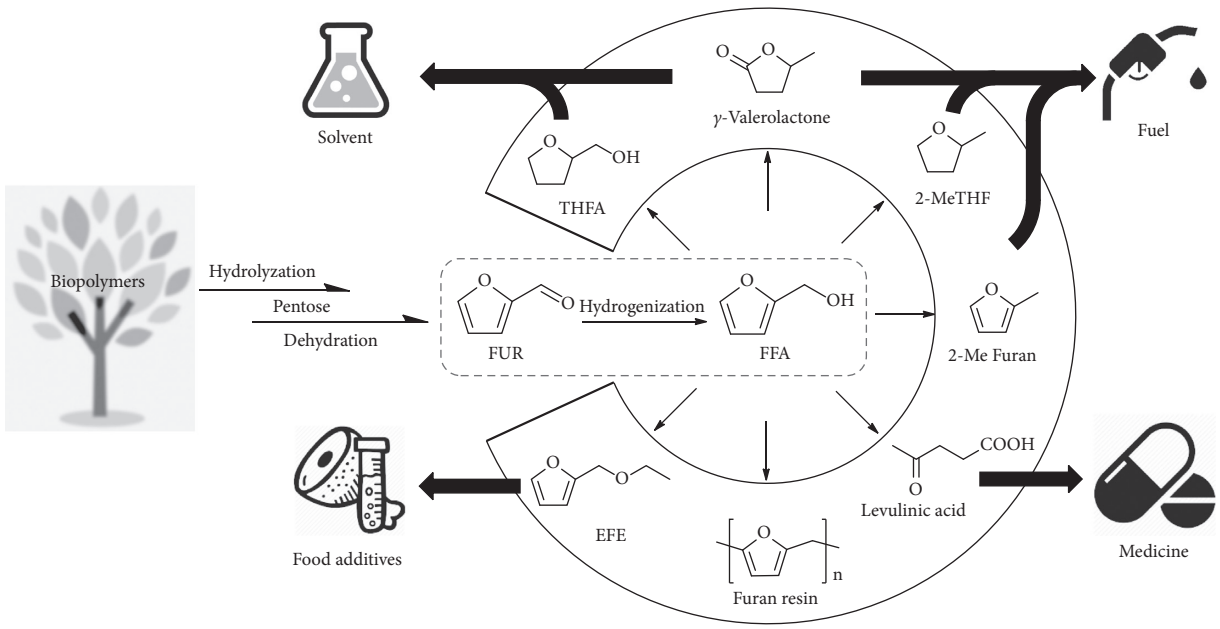

Figure 1: Biomass valorization by the hydrogenation of FUR to FFA. FUR: furfural; FFA: furfuryl alcohol; EFE: 2-(ethoxymethyl) furan; THFA: tetrahydrofurfuryl alcohol; 2-Me THF: 2-methyltetrahydrofuran; 2-MeFuran: 2-methylfuran.

Hydrogen gas as a gaseous H-donor has superiority in the product separation and thus is broadly applied in the diverse hydrogen reactions [32]. At room temperature, hydrogen gas is hard to react with other compounds until the reaction conditions change. High temperature and metal catalysts are effective for the activation of hydrogen gas. Thus, in industrial manufacture, the production of FFA from FUR and molecular hydrogen is completed at high temperatures catalyzed by noble metals (e.g., Au, Ru, Pd, and Pt) [33–36], nonnoble metals (e.g., Co, Cu, and Fe) [19, 37–40], and metallic oxides (e.g., $CrCuO_3$) [41]. However, due to the high activity of metal catalysts, aldehyde group and furan ring can be both reduced in this reaction system, resulting in that most catalysts used in the hydrogenation of FUR to FFA are still applied in the laboratory scale. In addition, with the reaction temperature exceeding the boiling point of FUR (167°C), FFA can be efficiently prepared from gas state FUR and hydrogen gas in atmospheric pressure, which indicates that the hydrogenation of FUR can react in both vapor state and liquid state. At the relatively low temperature, hydrosilane, alcohol, acid, and similar liquid compounds with free hydrogen atoms are good H-donor for hydrogenation of FUR to FFA in the liquid phase. The Meerwein–Ponndorf–Verley (MPV) reduction which is used alcohol as liquid H-donor has been largely applied in the reduction of biomass platform molecules, which can simultaneously produce two useful compounds and thus attracts the attention of numerous researchers focusing on biomass valorization [42–44]. Generally, the catalysts performing high catalytic activity for the MPV reduction of FUR to FFA include acid-base bifunctional catalysts (e.g., Pd/HZSM-5 and MgO-Al_2O_3) [45, 46] and Lewis acid catalysts (e.g., Al-, Zr-zeolites, and Zr-, Al-, Hf-based catalysts) [47–49]. It is noteworthy that the drawbacks of the MPV reaction system such as difficult separation of products and relatively harsh conditions still trouble researchers in this research field. Besides gas-phase H-donor hydrogen gas and alcohol H-donor, increasing reports about the hydrogenation of FUR to FFA by another liquid H-donor hydrosilane have been presented in the past decade [50, 51]. In this reaction system, FFA is obtained from FUR in high selectivity under mild conditions (atmospheric pressure, <80°C), which makes up the imperfection of the reaction system when hydrogen and alcohol are used as H-donor.

For hydrosilane, polymethylhydrosiloxane (PMHS) as the cheapest hydrosilane agent and the by-product of the silicon industry is an ideal H-donor for the hydrogenation of FUR to FFA [8, 52, 53]. At the same time, PMHS is a green agent as it is nontoxic and having great chemical stability for water and atmosphere [54, 55].

Recently, a series of fluoride salts were reported for the conversion of aldehyde to corresponding alcohol by PMHS in highly selective and effective environment [56, 57]. However, the fluoride salts as homogeneous catalysts are not suitable for economically manufacturing FFA from FUR, for which a novel and recyclable catalyst KF/support is reported in this article. The catalyst prepared by the impregnation method provides a suitable carrier for KF to attach, which is favorable for the contract of the substrate with KF and preventing KF from the erosion of solvent and substrate [32, 58]. Through the impregnation method, the obtained solid catalyst that combines the high efficiency of KF and the heterogeneous property of support was developed to catalyze the hydrogenation of FUR to FFA at a lower cost.

2. Results and Discussions

2.1. Effect of Different Supports. For the impregnation method, the loading amount of active sites on the solid support is generally decided by the support porosity and

chemical property [59]. Therefore, the influence of different porous supports on the catalytic behavior of KF was initially investigated (Figure 2). The loading rate of all support catalysts is 3 wt.%.

The results listed in Figure 2 show that KF supported on acidic montmorillonite K-10 (K-10) and alkaline hydroxyapatite microspheres (HAP) and nanomagnesium oxide (MgO) performed poor reactivity in this reaction system, which could be attributed to the ion exchange between the support with KF [60] or the competing reaction of fluoride ion and hydroxide released from the support [61], remarkably weakening the nucleophilic attack ability of KF. In connection with this, nanotitanium dioxide (TiO_2) and zirconium oxide nanopowder (ZrO_2) with both moderate acid and base sites supported KF showed relatively good catalytic activity for the conversion of FUR to FFA. In addition, due to the relatively high surface area of ZrO_2, the catalyst using ZrO_2 (75% FFA yield) as support had better catalytic reactivity than TiO_2 (55% FFA yield). Therefore, ZrO_2 which has both moderate acid and base sites and the relatively high surface area is the optimum support for catalyst KF/support.

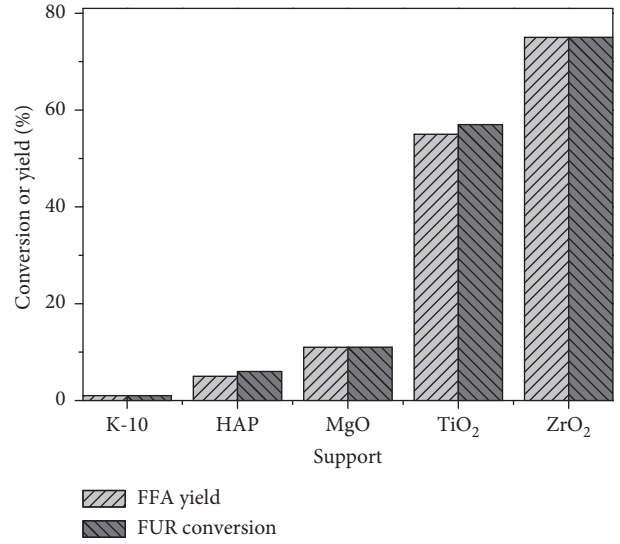

Figure 2: Effect of different supports on the synthesis of FFA from FUR. Reaction conditions: 0.5 mmol FUR, 25 mg catalyst, 2.5 equiv. H^- of PMHS, 2 mL DMF, 25°C, and 30 min. K-10: montmorillonite K-10; HAP: hydroxyapatite microspheres; MgO: nanomagnesium oxide; TiO_2: nanotitanium dioxide; ZrO_2: zirconium oxide nanopowder.

2.2. Effect of the Loading Rate of KF. Apart from the support, the loading rate of KF is another important factor for the catalyst preparation via impregnation [62]. The KF/ZrO_2 catalysts with different KF loading rates (1–15 wt.%) were prepared by the impregnation method for the test of catalytic activity (Figure 3). It was shown that 5 wt.% was the best loading rate of KF/ZrO_2 catalyst and increasing the loading rate of KF gave rise to the slight reduction of the catalyst activity of KF/support catalyst. For the decrease of catalytic activity of 15 wt.% KF/ZrO_2, this phenomenon could be attributed to the reduction of pore diameter which is caused by the excess of KF. To prove the inference, N_2 adsorption-desorption isotherms of KF/support in different loading rates are presented in Figure S3. The hysteresis loop appearing in the N_2 adsorption-desorption isotherms of 5 wt.% and 15 wt.% KF/ZrO_2 (Figure S3) is the phenomenon of decrease in pore diameter of 5 wt.% and 15 wt.% KF/ZrO_2 catalysts, proving the inference why the catalytic activity of 15 wt.% KF/ZrO_2 catalyst is declined.

Through the optimization of the support type and the loading content of KF, 5 wt.% KF/ZrO_2 shows the best catalytic activity for the hydrogenation of FUR to FFA. In addition, comparison of the results obtained in this work with those of previous studies for the conversion of FUR to FFA is presented in Table 1, which shows that 5 wt.% KF/ZrO_2 is a more efficient catalyst for the selective hydrogenation of FUR to FFA.

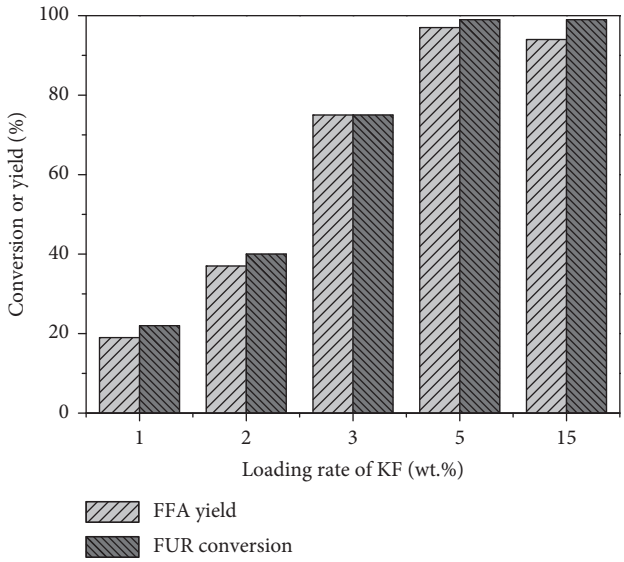

Figure 3: Effect of KF loading rate of KF/ZrO_2 on the reduction of FUR to FFA. Reaction conditions: 0.5 mmol FUR, 25 mg KF/ZrO_2, 2.5 equiv. H^- of PMHS, 2 mL DMF, 25°C, and 30 min.

2.3. Catalyst Characterization. The successful preparation of KF/ZrO_2 by the impregnation method commonly keeps the original configuration of support and makes the active substrate KF uniformly distributed in the internal surface of ZrO_2. According to the XRD patterns of KF/ZrO_2 catalysts with different KF loading rates (1–15 wt.%) (Figure 4), it can be seen that the crystal structure of ZrO_2 does not change significantly. The crystal faces of ZrO_2 including (1, 1, 0), (−1, 1, 1), (1, 1, 1), (1, 0, 2), (−2, 2, 1), (1, 3, 0), and (1, 3, 1) are attributed to the diffraction peaks at 24.1°, 27.9°, 31.4°, 34.1°, 40.8°, 50.4°, 55.3°, and 59.6°, respectively. As can be seen from the XPS spectra of 5 wt.% KF/ZrO_2 (Figure 5), the peaks of 690 eV and 290 eV that, respectively, correspond to the fluorine and potassium are detected, indicating that KF is successfully distributed in the external surface of the support. In the XRD pattern of KF/ZrO_2, the diffraction peak at 39.5° can be observed, manifesting the formation of the

Table 1: Catalytic results collected for the hydrogenation of FUR to FFA.

Catalyst	Temperature (°C)	Time (h)	H-donor	Yield (%)	Selectivity (%)	Reuse times (yield)	Ref.
Fe-L1/C-800	160	15	2-Butanol	75.87	82.9	5 (60.1%)	[44]
γ-Fe_2O_3@HAP	180	3	*iso*-Propanol	59.5	91.6	6 (57.2%)	[63]
Co/SBA-15	150	1.5	2 MPa H_2	87.6	95.6	11 (50.5%)	[64]
5 wt.% Ni/CN	200	4	1 MPa H_2	91.4	95.0	4 (91.4%)	[65]
CuCo0.4/C-873	140	1	3 MPa H_2	28.5	93.4	4 (17.4%)	[66]
5 wt.% KF/ZrO_2	25	0.5	PMHS	97.0	98.0	5 (71%)	This work

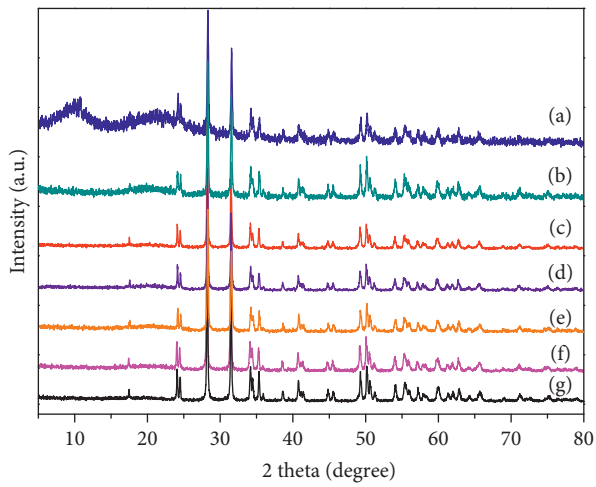

Figure 4: XRD patterns of (a) 5 wt.% KF/ZrO_2 (after recycling 5 times), (b) 15 wt.% KF/ZrO_2, (c) 5 wt.% KF/ZrO_2, (d) 3 wt.% KF/ZrO_2, (e) 2 wt.% KF/ZrO_2, (f) 1 wt.% KF/ZrO_2, and (g) ZrO_2.

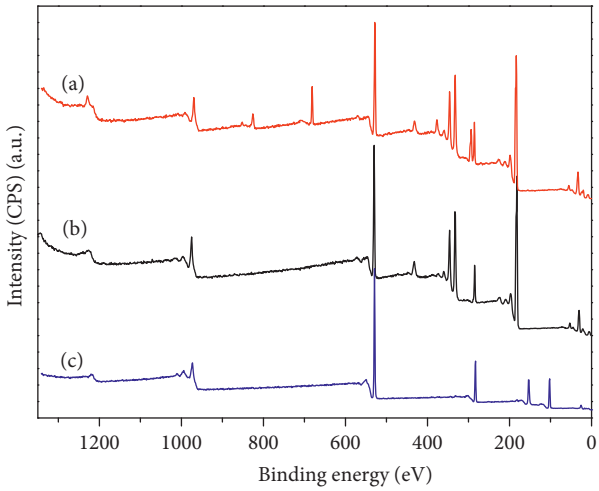

Figure 5: XPS profiles of (a) 5 wt.% KF/ZrO_2, (b) ZrO_2, and (c) 5 wt.% KF/ZrO_2 (after recycling 5 times).

alkaline active species ($K_3Zr_2F_{11}$) by the chemical combination of K^+ and oxygen species [67]. The results show that KF is immobilized on ZrO_2 which is realized by both physical adsorption and chemical interaction. It is known that ZrO_2 as a porous material has a relatively large surface area (ca. 80–110 m^2/g), most of which is provided by the internal surface [68, 69]. Through comparison of the detection results obtained by XPS and ICP-MS analysis (Table 2), a relatively high K content of KF/ZrO_2 detected by ICP indicated that KF is successfully distributed in both the external and internal surface of ZrO_2. In addition, the thermostability of catalysts was detected by TG analysis, and the results show that the quality of KF/ZrO_2 is very stable, in which the catalyst weight is slightly decreased when the calcination temperature increases from 25 to 600°C.

2.4. Effect of Different Solvents. Five kinds of solvents were chosen for comparing the effect of different solvents on the reduction of FUR to FFA (Figure 6). For the protic solvent, methanol (MeOH) or *n*-butanol (*n*-BuOH) used as solvent showed relatively low reactivity (6% or 43% FFA yield and 11% or 44% FUR conversion, respectively). It was proposed that alcohol could react with PMHS to produce hydrogen gas [70], significantly decreasing the amount of PMHS for the reduction of FUR, which thus afforded lower FFA yield and FUR conversion. For the aprotic solvent, the order of reactivity is correlated with the order of the solvent polarity: *N*,*N*-dimethylformamide (DMF) > ethyl acetate (EA) > 2-methylfuran (2-MeTHF) (Figure 6). DMF as the relatively high polarity solvent shows the best FFA yield (97%) and FUR conversion (99%), for which DMF was considered as the optimum solvent for this reaction system.

2.5. Effect of PMHS Dosage and Hydrosilane Type. Effect of PMHS dosage was investigated from 0.5 to 4 equiv. at intervals of 0.5 equiv. (Figure 7). It was obvious that the low dosage of PMHS could not provide enough H-donor to complete the reduction of FUR to FFA and the excess dosage of PMHS against the dissociation between FFA and PMHS, thus reducing the yield of FFA [71]. PMHS with 2.5 equiv. H^- was found to be the optimum dosage of PMHS, which is in favor of the FUR to FFA hydrogenation in an economical and efficient way.

After confirming the optimum dosage of PMHS, there are eight kinds of hydrosilanes that are used for the study of hydrosilane type effect (Table 3). For the hydrosilanes containing phenyl species, phenylsilane (PS) and diphenylsilane (DPS) showed very good activity in the reduction of FUR to FFA, giving FFA yield in >99% or 99.0%, respectively. For the hydrosilanes not containing phenyl species, 99% FFA yield could be obtained using PMHS as H-donor, which is the highest FFA yield (1–75%) among the hydrosilanes not containing phenyl groups. From the point of economy, although using hydrosilanes containing phenyl groups as H-donor achieved high FFA yields, the price of PS and DPS is 72 and 38 times higher than that of PMHS,

Table 2: Composition of the fresh and reused catalysts detected by XPS and ICP analysis.

Entry	Detection method	Sample	K (mol%)	F (mol%)
1	ICP	5 wt.% KF/ZrO_2	3.58	—
2	ICP	Reused 5 wt.% KF/ZrO_2	3.02	—
3	XPS	5 wt.% KF/ZrO_2	2.99	3.79
4	XPS	Reused 5 wt.% KF/ZrO_2	0.01	0.01

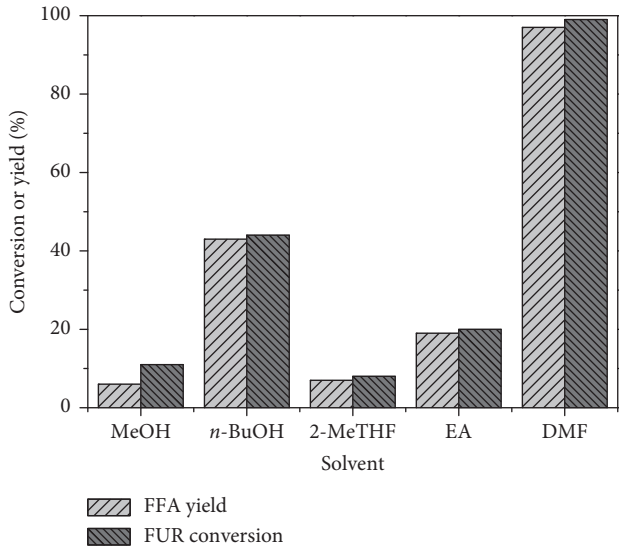

Figure 6: Influence of solvent type on the hydrogenation of FUR to FFA. Reaction conditions: 0.5 mmol FUR, 25 mg 5 wt.% KF/ZrO_2, 2.5 equiv. H^- of PMHS, 2 mL solvent, 25°C, and 30 min. DMF: *N*,*N*-dimethylformamide; EA: ethyl acetate; 2-MeTHF: 2-methylfuran; MeOH: methanol; *n*-BuOH: *n*-butanol.

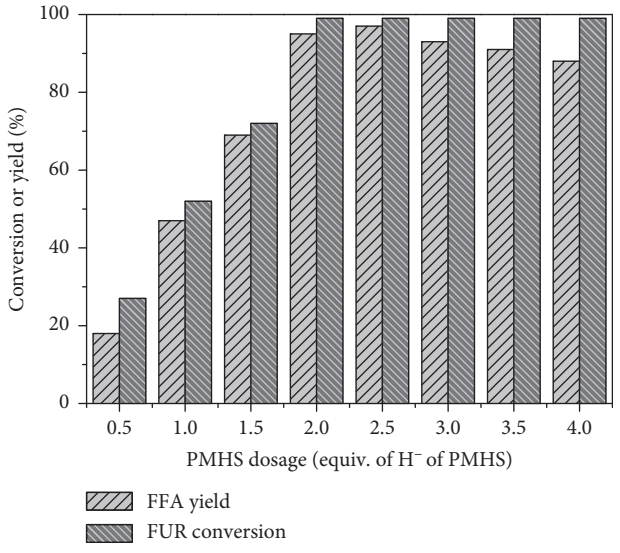

Figure 7: Effect of PMHS dosage on the reduction of FUR to FFA. Reaction conditions: 0.5 mmol FUR, 25 mg 5 wt.% KF/ZrO_2, 2 mL DMF, 25°C, and 30 min.

respectively [50], which is too expensive to carry out for practical application. As the cheapest hydrosilane, PMHS performed relatively high FFA yield (99%) as well, for which PMHS is considered as the optimum hydrosilane from the examined hydrosilanes.

2.6. Catalyst Recycling Study. The reusability of 5 wt.% KF/ZrO_2 was also investigated, and the obtained results are shown in Figure 8. After five consecutive runs, the FFA yield marginally decreased from 97% to 71%.

From the XRD pattern of reused 5 wt.% KF/ZrO_2 catalyst, it was revealed that the crystallization of the catalyst was decreased after recycles (Figure 4). Thus, the reason why the catalyst activity is slightly decreased could be attributed to the catalyst pore blocking by the PMHS-based resin, which is a typical by-product of reaction system using PMHS as H-donor [72]. To prove the reasonability of the inference, the characterizations of reused 5 wt.% KF/ZrO_2 by SEM, BET, XPS, and ICP-MS are conducted. Firstly, from the SEM image of the reused catalyst (Figure S1), it can be seen that the surface of the catalyst is covered by an unknown substrate. For the XPS spectra of reused 5 wt.% KF/ZrO_2 (Figure 5), the characteristic peak of silicon (102 eV) was detected, indicating that 5 wt.% KF/ZrO_2 is covered by PMHS-based resin. The BET isotherms and pore diameter analysis suggest that the pore diameter is reduced after use (Figures S2 and S3). Thus, the PMHS-based resin that is wrapping the 5 wt.% KF/ZrO_2 restricts the substrate to enter into the cavity of support, which decreases the contact of active compounds to substrate and weakens the catalytic activity of 5 wt.% KF/ZrO_2. Meanwhile, the sharp decrease of KF content is also attributed to the coverage of PMHS resin, which can be illustrated by the significant peak of silicon in the XPS spectrum (Figure 5). Except the effect of PMHS-

Table 3: Influence of hydrosilane type on the reduction of FUR to FFA.

Entry	Hydrosilane structure	Chemical name	Yield (%)	Conversion (%)	Selectivity (%)
1	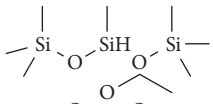	1,1,1,3,5,5,5-Heptamethyltrisiloxane	72	>99	72
2	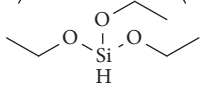	Triethoxysilane	75	>99	75
3	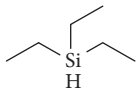	Triethylsilane	1	5	20
4	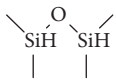	1,1,3,3-Tetramethyldisiloxane	>99	>99	100
5	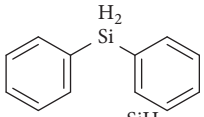	Diphenylsilane	99	>99	99
6	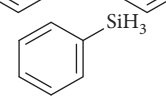	Phenylsilane	>99	>99	100
7	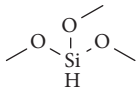	Trimethoxysilane	57	88	65
8	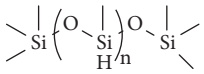	PMHS	97	99	98

Reaction conditions: 0.5 mmol FUR, 25 mg 5 wt.% KF/ZrO_2, 2 mL DMF, 2.5 equiv. H^- of hydrosilane, 25°C, and 30 min.

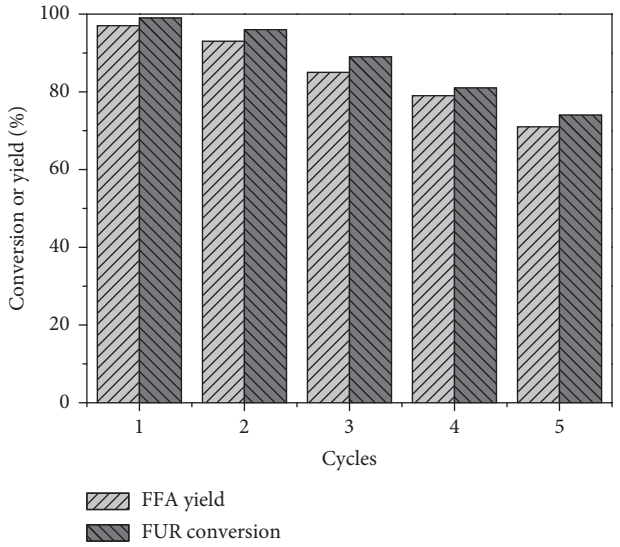

Figure 8: Catalyst recycling study of 5 wt.% KF/ZrO_2. Reaction conditions: 0.5 mmol FUR, 25 mg 5 wt.% KF/ZrO_2, 2 mL DMF, 2.5 equiv. H^- of PMHS, 25°C, and 30 min.

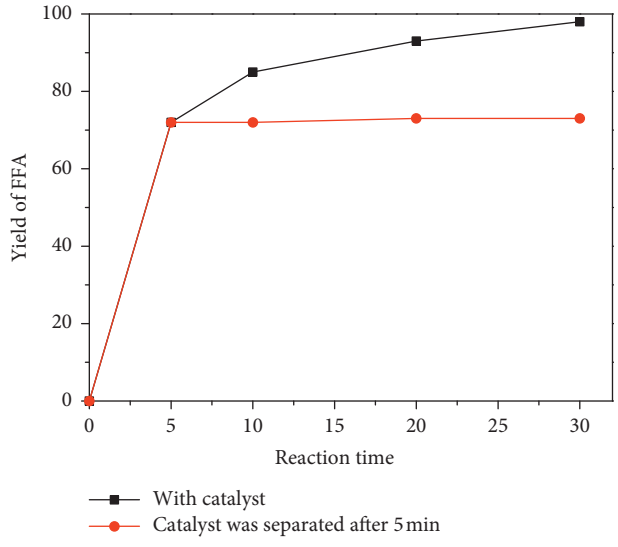

Figure 9: The FFA yield with or without the participation of 5 wt.% KF/ZrO_2. Reaction conditions: 0.5 mmol FUR, 25 mg 5 wt.% KF/ZrO_2, 2 mL DMF, 2.5 equiv. H^- of PMHS, 25°C, and 30 min.

based resin, the slight loss of KF is another factor for the decrease in the catalytic activity of 5 wt.% KF/ZrO_2 after use. The atomic analysis of fresh and reused 5 wt.% KF/ZrO_2 catalyst by ICP-MS (Table 2) indicates that KF was not significantly leached (by ca, 0.56%). Meanwhile, the hot filtration experiments (Figure 9) confirm the heterogeneous catalytic behavior of the solid catalyst. Therefore, the main factor that decreases the catalytic activity is the PMHS resin which covers the external surface of 5 wt.% KF/ZrO_2.

3. Conclusion

In summary, the KF/ZrO_2 catalyst was successfully prepared by the impregnation method and had good reactivity for the

reduction of FUR to FFA using PMHS as H-donor. For the support of the catalyst, ZrO_2 as a porosity material of chemical inertness maintains the original configuration after the process of impregnation. Meanwhile, 5 wt.% KF/ZrO_2 as an appropriate loading rate of KF keeps the porosity of support and high reactivity of KF. The benign reaction system was optimized, and thus, 97% FFA yield and 99% FUR conversion were achieved by this reaction system at 25°C after 0.5 h. Through the comparison of seven kinds of commercial hydrosilanes and PMHS, PMHS is considered as hydrosilane of the high price-performance ratio. The reusability of 5 wt.% KF/ZrO_2 is good, which further reduced the cost of the reaction system. After 5 times run, the FFA yield was slightly decreased from 97% to 71%, due to the pore of 5 wt.% KF/ZrO_2 covered by PMHS-based resin.

4. Materials and Experiments

4.1. Materials. Polymethylhydrosiloxane (>99.0%), potassium fluoride (>99.9%), 2-methylfuran (>99.9%), 1,1,3,3-tetramethyldisiloxane (>98.0%), nanotitanium dioxide (>99.8%), hydroxyapatite microspheres, and naphthalene (>99.0%) were purchased from Shanghai Aladdin Bio-Chem Technology Co., Ltd. Triethoxysilane (>97.0%), 1,1,1,3,5,5,5-heptamethyltrisiloxane (>98.0%), triethylsilane (>98.0%), trimethoxysilane (>95.0%), and phenylsilane (>97.0%) were bought from Tokyo Chemical Industry Co., Ltd. *N*,*N*-Dimethylformamide (>99.5%), methanol (>99.5%), and tetrahydrofuran (>99.5%) were purchased from Guangdong Guanghua Sci-Tech Co., Ltd. *n*-Butanol (>99.5%) and ethyl acetate (>99.5%) were obtained from Shanghai Shenbo Chemical Co., Ltd. Diphenylsilane (>97.0%) and zirconium dioxide nanopowder (>99.5%) were purchased from Alfa Aesar Chemicals Co., Ltd. Nanomagnesium oxide (>99.0%), montmorillonite K-10, and others were purchased from Beijing Innochem Technology Co., Ltd.

4.2. Preparation of Catalyst. A series of KF/support catalysts were prepared through an impregnation method. KF solution was prepared at first, where a desired amount of KF was dissolved into 2 mL pure water. Then, 1 g support was added into the solution. The mixture was heated at 60°C with stirring for 6 h. Finally, the mixture was dried at 80°C for 12 h, and the catalyst was ground for the test of catalytic activity. Through the impregnation method, active compound KF was distributed in the internal and external surface of the support by two steps. First, the support is completely immersed in the solution containing a moderate amount of KF until the cavity of support is full of KF solution by capillarity. Second, through a drying process, the solvent in the KF solution is completely volatilized, making the active compound KF be attached to the support surface.

4.3. Catalyst Characterization Techniques. BET (Brunauer–Emmett–Teller) surface areas of the porous materials were determined from nitrogen physisorption measurements at liquid nitrogen temperature on a Micromeritics ASAP 2460 instrument. Scanning electron microscopy (SEM) images were obtained by using field-emission scanning electron microscopy (FESEM; JEOL, EOL, JSM-6700F, 5 kV). Thermogravimetry (TG) analysis was determined by a NETZSCH STA 449 F3 Jupiter. XPS (X-ray photoelectron spectroscopy) measurements were recorded using a Physical Electronics Quantum 2000 Scanning ESCA Microprobe (Physical Electronics Inc., PHI, MN) equipped with a monochromatic Al Kα anode. The data of XRD (X-ray diffraction) of the powder samples were obtained by using a Rigaku International D/max-TTR III X-ray powder diffractometer with Cu Kα radiation and 2θ scanned from 5° to 80°. The quantitative elemental analysis of samples was completed by coupled plasma mass spectrometry (ICP-MS, Elan DRC II, PerkinElmer, Sciex).

4.4. Catalytic Transfer Hydrogenation. A plastic sealed tube is a vessel where the FFA hydrogenation reaction was carried out. In a general process, FUR (0.5 mmol, 0.048 g), KF/ZrO_2 (25 mg), DMF (2 mL), and PMHS were added successively into a 15 mL plastic tube and then the lid was covered. Afterward, the sealed tube filling with the reaction mixture was put into the oil bath that was kept at 25°C. Upon completion, methanol (2 mL) was added to quench the reaction, and the reaction mixture was filtered by a 0.2 μm filter membrane for GC analysis.

4.5. Product Analysis. The quantitative analysis of the reaction mixture was fulfilled by GC (Agilent 6890N) equipped with an HP-5 capillary column (30 m × 0.320 mm × 0.25 μm) and flame ionization detector (FID) detector. The programmed temperature for GC analysis is set as follows: maintaining at 60°C for 1 min, heating from 60 to 230°C in the rate of 10°C/min, and holding for 4 min. Naphthalene was employed as an internal standard for the quantitative analysis of the samples. The standard curves of FUR and FFA were recorded with GC by plotting different concentrations of FUR or FFA with specific concentrations of naphthalene, and the obtained curves are shown in Figures S5 and S6. The substrate conversion and product yield are calculated using the following equations, based on the standard curves made from commercial samples:

$$\text{conversion } (\%) = \left(1 - \frac{\text{mole of residual substrate}}{\text{mole of initial substrate}}\right) \times 100\%,$$

$$\text{yield } (\%) = \frac{\text{mole of product}}{\text{mole of initial substrate}} \times 100\%. \quad (1)$$

Data Availability

The data used to support the findings of this study are available from the corresponding author upon request.

Conflicts of Interest

The authors declare no conflicts of interest.

Authors' Contributions

Zhaozhuo Yu and Weibo Wu contributed equally to this work.

Acknowledgments

This study was financially supported by the National Natural Science Foundation of China (21576059, 21666008, and 21908033), Fok Ying-Tong Education Foundation (161030), Key Technologies R&D Program of China (2014BAD23B01), and Guizhou Science and Technology Foundation ([2018] 1037).

Supplementary Materials

SEM images (Figure S1), pore distribution (Figure S2), N2 adsorption-desorption isotherms (Figure S3), and TG curves (Figure S4) of solid catalysts, as well as standard curves of FUR (Figure S5) and FFA (Figure S6) are provided. (*Supplementary Materials*)

References

[1] H. Li, S. Yang, A. Riisager et al., "Zeolite and zeotype-catalysed transformations of biofuranic compounds," *Green Chemistry*, vol. 18, no. 21, pp. 5701–5735, 2016.

[2] K. Shikinaka, H. Sotome, Y. Kubota et al., "A small amount of nanoparticulated plant biomass, lignin, enhances the heat tolerance of poly(ethylene carbonate)," *Journal of Materials Chemistry A*, vol. 6, no. 3, pp. 837–839, 2018.

[3] S. Xu, M. E. Lamm, M. A. Rahman et al., "Renewable atom-efficient polyesters and thermosetting resins derived from high oleic soybean oil," *Green Chemistry*, vol. 20, no. 5, pp. 1106–1113, 2018.

[4] A. R. Alcantara and P. D. de Maria, "Recent advances on the use of 2-methyltetrahydrofuran (2-MeTHF) in biotransformations," *Current Green Chemistry*, vol. 5, no. 2, pp. 86–103, 2018.

[5] G. W. Huber, J. N. C. Huber, J. Christopher, and J. A. Barrett, "Production of liquid alkanes by aqueous-phase processing of biomass-derived carbohydrates," *Science*, vol. 308, no. 5727, pp. 1446–1450, 2005.

[6] D. Zhang, J. Wang, Y. Lin et al., "Present situation and future prospect of renewable energy in China," *Renewable and Sustainable Energy Reviews*, vol. 76, pp. 865–871, 2017.

[7] T. Wangchuk, C. He, L. D. Knibbs, M. Mazaheri, and L. Morawska, "A pilot study of traditional indoor biomass cooking and heating in rural Bhutan: gas and particle concentrations and emission rates," *Indoor Air*, vol. 27, no. 1, pp. 160–168, 2017.

[8] H. Li, W. Zhao, W. Dai et al., "Noble metal-free upgrading of multi-unsaturated biomass derivatives at room temperature: silyl species enable reactivity," *Green Chemistry*, vol. 20, no. 23, pp. 5327–5335, 2018.

[9] S. Saravanamurugan, A. Riisager, E. Taarning, and S. Meier, "Mechanism and stereoselectivity of zeolite-catalysed sugar isomerisation in alcohols," *Chemical Communications*, vol. 52, no. 86, pp. 12773–12776, 2016.

[10] F. H. Isikgor and C. R. Becer, "Lignocellulosic biomass: a sustainable platform for the production of bio-based chemicals and polymers," *Polymer Chemistry*, vol. 6, no. 25, pp. 4497–4559, 2015.

[11] C. Xu, R. A. D. Arancon, J. Labidi, and R. Luque, "Lignin depolymerisation strategies: towards valuable chemicals and fuels," *Chemical Society Reviews*, vol. 43, no. 22, pp. 7485–7500, 2014.

[12] M. J. Gilkey and B. Xu, "Heterogeneous catalytic transfer hydrogenation as an effective pathway in biomass upgrading," *ACS Catalysis*, vol. 6, no. 3, pp. 1420–1436, 2016.

[13] R. A. Sheldon, "Green and sustainable manufacture of chemicals from biomass: state of the art," *Green Chemistry*, vol. 16, no. 3, pp. 950–963, 2014.

[14] J.-P. Lange, E. van der Heide, J. van Buijtenen, and R. Price, "Furfural-A promising platform for lignocellulosic biofuels," *ChemSusChem*, vol. 5, no. 1, pp. 150–166, 2012.

[15] R. Mariscal, P. Maireles-Torres, M. Ojeda, I. Sádaba, and M. López Granados, "Furfural: a renewable and versatile platform molecule for the synthesis of chemicals and fuels," *Energy & Environmental Science*, vol. 9, no. 4, pp. 1144–1189, 2016.

[16] Z. Liu, D. Tian, J. Hu et al., "Functionalizing bottom ash from biomass power plant for removing methylene blue from aqueous solution," *Science of the Total Environment*, vol. 634, pp. 760–768, 2018.

[17] R. Jia, H. Lei, T. Hino, and A. Arulrajah, "Environmental changes in Ariake Sea of Japan and their relationships with Isahaya Bay reclamation," *Marine Pollution Bulletin*, vol. 135, pp. 832–844, 2018.

[18] G. D. Oreggioni, B. Singh, F. Cherubini et al., "Environmental assessment of biomass gasification combined heat and power plants with absorptive and adsorptive carbon capture units in Norway," *International Journal of Greenhouse Gas Control*, vol. 57, pp. 162–172, 2017.

[19] K. Yan and A. Chen, "Efficient hydrogenation of biomass-derived furfural and levulinic acid on the facilely synthesized noble-metal-free Cu–Cr catalyst," *Energy*, vol. 58, pp. 357–363, 2013.

[20] J. Wang, Z. Zhang, S. Jin, and X. Shen, "Efficient conversion of carbohydrates into 5-hydroxylmethylfurfan and 5-ethoxymethylfurfural over sufonic acid-functionalized mesoporous carbon catalyst," *Fuel*, vol. 192, pp. 102–107, 2017.

[21] C. Fang, Y. Li, Z. Yu, H. Li, and S. Yang, "Efficient catalytic upgrade of fructose to alkyl levulinates with phenylpyridine-phosphotungstate solid hybrids," *Current Green Chemistry*, vol. 6, no. 1, pp. 44–52, 2019.

[22] D. Darji, Y. Alias, and N. H. Abd Razak, "Effect of recycled imidazolium-based ionic liquids on biomass from rubber wood," *Current Green Chemistry*, vol. 4, pp. 74–81, 2017.

[23] H. Li, S. Saravanamurugan, S. Yang, and A. Riisager, "Direct transformation of carbohydrates to the biofuel 5-ethoxymethylfurfural by solid acid catalysts," *Green Chemistry*, vol. 18, no. 3, pp. 726–734, 2016.

[24] S. Zhang, M. Yang, J. Shao et al., "The conversion of biomass to light olefins on Fe-modified ZSM-5 catalyst: effect of pyrolysis parameters," *Science of The Total Environment*, vol. 628-629, pp. 350–357, 2018.

[25] R. Luque, "Catalytic biomass processing: prospects in future biorefineries," *Current Green Chemistry*, vol. 2, no. 1, pp. 90–95, 2015.

[26] H. Li, T. Yang, and Z. Fang, "Biomass-derived mesoporous Hf-containing hybrid for efficient Meerwein-Ponndorf-Verley reduction at low temperatures," *Applied Catalysis B: Environmental*, vol. 227, pp. 79–89, 2018.

[27] L. Filiciotto and R. Luque, "Biomass promises: a bumpy road to a renewable economy," *Current Green Chemistry*, vol. 5, no. 1, pp. 47–59, 2018.

[28] K. T. Malladi and T. Sowlati, "Biomass logistics: a review of important features, optimization modeling and the new trends," *Renewable and Sustainable Energy Reviews*, vol. 94, pp. 587–599, 2018.

[29] D. M. Alonso, S. G. Wettstein, and J. A. Dumesic, "Bimetallic catalysts for upgrading of biomass to fuels and chemicals," *Chemical Society Reviews*, vol. 41, no. 24, pp. 8075–8098, 2012.

[30] L. Zhang, G. Xi, K. Yu, H. Yu, and X. Wang, "Furfural production from biomass-derived carbohydrates and lignocellulosic residues via heterogeneous acid catalysts," *Industrial Crops and Products*, vol. 98, pp. 68–75, 2017.

[31] L. Zhang, G. Xi, Z. Chen, D. Jiang, H. Yu, and X. Wang, "Highly selective conversion of glucose into furfural over modified zeolites," *Chemical Engineering Journal*, vol. 307, pp. 868–876, 2017.

[32] W. Gong, C. Chen, Y. Zhang et al., "Efficient synthesis of furfuryl alcohol from H2-hydrogenation/transfer hydrogenation of furfural using sulfonate group modified Cu catalyst," *ACS Sustainable Chemistry & Engineering*, vol. 5, no. 3, pp. 2172–2180, 2017.

[33] Y. Nakagawa, K. Takada, M. Tamura, and K. Tomishige, "Total hydrogenation of furfural and 5-hydroxymethylfurfural over supported Pd-Ir alloy catalyst," *ACS Catalysis*, vol. 4, no. 8, pp. 2718–2726, 2014.

[34] Q. Yuan, D. Zhang, L. v. Haandel et al., "Selective liquid phase hydrogenation of furfural to furfuryl alcohol by Ru/Zr-MOFs," *Journal of Molecular Catalysis A: Chemical*, vol. 406, pp. 58–64, 2015.

[35] W. Huang, H. Li, B. Zhu, Y. Feng, S. Wang, and S. Zhang, "Selective hydrogenation of furfural to furfuryl alcohol over catalysts prepared via sonochemistry," *Ultrasonics Sonochemistry*, vol. 14, no. 1, pp. 67–74, 2007.

[36] S. Sitthisa and D. E. Resasco, "Hydrodeoxygenation of furfural over supported metal catalysts: a comparative study of Cu, Pd and Ni," *Catalysis Letters*, vol. 141, no. 6, pp. 784–791, 2011.

[37] V. Vetere, A. B. Merlo, J. F. Ruggera, and M. L. Casella, "Transition metal-based bimetallic catalysts for the chemoselective hydrogenation of furfuraldehyde," *Journal of the Brazilian Chemical Society*, vol. 21, no. 5, pp. 914–920, 2010.

[38] S. Sanjay, S. Naveen, M. Pravakar, K. A. Shah, J. K. Parikh, and D. Ajay K, "Optimization and kinetic studies on hydrogenation of furfural to furfuryl alcohol over SBA-15 supported bimetallic copper–cobalt catalyst," *Catalysis Letters*, vol. 145, no. 3, pp. 816–823, 2015.

[39] K. Yan, J. Liao, X. Wu, and X. Xie, "A noble-metal free Cu-catalyst derived from hydrotalcite for highly efficient hydrogenation of biomass-derived furfural and levulinic acid," *RSC Advances*, vol. 3, no. 12, pp. 3853–3856, 2013.

[40] R. V. Sharma, U. Das, R. Sammynaiken, and A. K. Dalai, "Liquid phase chemo-selective catalytic hydrogenation of furfural to furfuryl alcohol," *Applied Catalysis A: General*, vol. 454, pp. 127–136, 2013.

[41] R. Rao, A. Dandekar, R. T. K. Baker, and M. A. Vannice, "Properties of copper chromite catalysts in hydrogenation reactions," *Journal of Catalysis*, vol. 171, no. 2, pp. 406–419, 1997.

[42] H. Li, Y. Li, Z. Fang, and R. L. Smith, "Efficient catalytic transfer hydrogenation of biomass-based furfural to furfuryl alcohol with recycable Hf-phenylphosphonate nanohybrids," *Catalysis Today*, vol. 319, pp. 84–92, 2019.

[43] H. Li, W. Zhao, S. Saravanamurugan et al., "Control of selectivity in hydrosilane-promoted heterogeneous palladium-catalysed reduction of furfural and aromatic carboxides," *Communications Chemistry*, vol. 1, p. 32, 2018.

[44] J. Li, J.-l. Liu, H.-j. Zhou, and Y. Fu, "Catalytic transfer hydrogenation of furfural to furfuryl alcohol over nitrogen-doped carbon-supported iron catalysts," *ChemSusChem*, vol. 9, no. 11, pp. 1339–1347, 2016.

[45] H. Li, J. He, A. Riisager, S. Saravanamurugan, B. Song, and S. Yang, "Acid-base bifunctional zirconium *N*-alkyl-triphosphate nanohybrid for hydrogen transfer of biomass-derived carboxides," *ACS Catalysis*, vol. 6, no. 11, pp. 7722–7727, 2016.

[46] A. Martínez, M. A. Arribas, M. Derewinski, and A. Burkat-Dulak, "Enhanced sulfur resistance of bifunctional Pd/HZSM-5 catalyst comprising hierarchical carbon-templated zeolite," *Applied Catalysis A: General*, vol. 379, no. 1-2, pp. 188–197, 2010.

[47] Y. Zhu, G. Chuah, and S. Jaenicke, "Chemo- and regioselective Meerwein-Ponndorf-Verley and Oppenauer reactions catalyzed by Al-free Zr-zeolite beta," *Journal of Catalysis*, vol. 227, no. 1, pp. 1–10, 2004.

[48] M. De bruyn, M. Limbourg, J. Denayer et al., "Mesoporous Zr and Hf catalysts for chemoselective MPV reductions of unsaturated ketones," *Applied Catalysis A: General*, vol. 254, no. 2, pp. 189–201, 2003.

[49] Y. Zhu, G. Chuah, and S. Jaenicke, "Selective Meerwein–Ponndorf–Verley reduction of α, $\beta\alpha$, β-unsaturated aldehydes over Zr-zeolite beta," *Journal of Catalysis*, vol. 241, no. 1, pp. 25–33, 2006.

[50] D. Addis, S. Das, K. Junge, and M. Beller, "Selective reduction of carboxylic acid derivatives by catalytic hydrosilylation," *Angewandte Chemie International Edition*, vol. 50, no. 27, pp. 6004–6011, 2011.

[51] V. Bette, A. Mortreux, D. Savoia, and J.-F. Carpentier, "New developments in zinc-catalyzed asymmetric hydrosilylation of ketones with PMHS," *Tetrahedron*, vol. 60, no. 12, pp. 2837–2842, 2004.

[52] Z. Yu, F. Xu, Y. Li, H. Konno, H. Li, and S. Yang, "Tetraethylammonium fluoride-mediated a green hydrogen transfer process for selective reduction of biomass-derived aldehydes," *Current Green Chemistry*, vol. 6, no. 2, pp. 127–134, 2019.

[53] H. Li, W. Zhao, A. Riisager et al., "A Pd-Catalyzed in situ domino process for mild and quantitative production of 2,5-dimethylfuran directly from carbohydrates," *Green Chemistry*, vol. 19, no. 9, pp. 2101–2106, 2017.

[54] H. Li, W. Zhao, and Z. Fang, "Hydrophobic Pd nanocatalysts for one-pot and high-yield production of liquid furanic biofuels at low temperatures," *Applied Catalysis B: Environmental*, vol. 215, pp. 18–27, 2017.

[55] E. Vasilikogiannaki, I. Titilas, C. Gryparis, A. Louka, I. N. Lykakis, and M. Stratakis, "Efficient hydrosilylation of carbonyl compounds by 1,1,3,3-tetramethyldisiloxane catalyzed by Au/TiO_2," *Tetrahedron*, vol. 70, no. 36, pp. 6106–6113, 2014.

[56] E. Abele and E. Lukevics, "Recent advances in fluoride ion activation of silicon bonds in organic synthesis," *Main Group Metal Chemistry*, vol. 24, no. 6, p. 315, 2001.

[57] M. D. Drew, N. J. Lawrence, W. Watson, and S. A. Bowles, "The asymmetric reduction of ketones using chiral ammonium fluoride salts and silanes," *Tetrahedron Letters*, vol. 38, no. 33, pp. 5857–5860, 1997.

[58] S. R. Mirmasoomi, M. Mehdipour Ghazi, and M. Galedari, "Photocatalytic degradation of diazinon under visible light using TiO_2/Fe_2O_3 nanocomposite synthesized by ultrasonic-assisted impregnation method," *Separation and Purification Technology*, vol. 175, pp. 418–427, 2017.

[59] M. Shimokawabe, H. Asakawa, and N. Takezawa, "Characterization of copper/zirconia catalysts prepared by an impregnation method," *Applied Catalysis*, vol. 59, no. 1, pp. 45–58, 1990.

[60] J. H. Clark, "Fluoride ion as a base in organic synthesis," *Chemical Reviews*, vol. 80, no. 5, pp. 429–452, 1980.

[61] K. Revunova and G. I. Nikonov, "Base-catalyzed hydrosilylation of ketones and esters and insight into the mechanism," *Chemistry-A European Journal*, vol. 20, no. 3, pp. 839–845, 2014.

[62] J. A. Korpiel and R. D. Vidic, "Effect of sulfur impregnation method on activated carbon uptake of gas-phase mercury," *Environmental Science & Technology*, vol. 31, no. 8, pp. 2319–2325, 1997.

[63] F. Wang and Z. Zhang, "Catalytic transfer hydrogenation of furfural into furfuryl alcohol over magnetic γ-Fe_2O_3@HAP catalyst," *ACS Sustainable Chemistry & Engineering*, vol. 5, no. 1, pp. 942–947, 2017.

[64] M. Audemar, C. Ciotonea, K. De Oliveira Vigier et al., "Selective hydrogenation of furfural to furfuryl alcohol in the presence of a recyclable cobalt/SBA-15 catalyst," *ChemSusChem*, vol. 8, no. 11, pp. 1885–1891, 2015.

[65] T. V. Kotbagi, H. R. Gurav, A. S. Nagpure, S. V. Chilukuri, and M. G. Bakker, "Highly efficient nitrogen-doped hierarchically porous carbon supported Ni nanoparticles for the selective hydrogenation of furfural to furfuryl alcohol," *RSC Advances*, vol. 6, no. 72, pp. 67662–67668, 2016.

[66] Y. Wang, Y. Miao, S. Li, L. Gao, and G. Xiao, "Metal-organic frameworks derived bimetallic Cu-Co catalyst for efficient and selective hydrogenation of biomass-derived furfural to furfuryl alcohol," *Molecular Catalysis*, vol. 436, pp. 128–137, 2017.

[67] H. Tang, Y. Li, N. Liu, L. Fu, and Y. Liu, "A highly-efficient KF-modified nanorod support Zr–Ce oxide catalyst and its application," *ChemCatChem*, vol. 10, no. 20, pp. 4739–4746, 2018.

[68] X. Yan, Q. Zhang, M. Zhu, and Z. Wang, "Selective hydrogenation of benzene to cyclohexene over Ru-Zn/ZrO_2 catalysts prepared by a two-step impregnation method," *Journal of Molecular Catalysis A: Chemical*, vol. 413, pp. 85–93, 2016.

[69] B. Sathyaseelan, E. Manikandan, I. Baskaran et al., "Studies on structural and optical properties of ZrO_2 nanopowder for opto-electronic applications," *Journal of Alloys and Compounds*, vol. 694, pp. 556–559, 2017.

[70] E. Lukevics and M. Dzintara, "The alcoholysis of hydrosilanes," *Journal of Organometallic Chemistry*, vol. 295, no. 3, pp. 265–315, 1985.

[71] J. Lipowitz and S. A. Bowman, "Use of polymethylhydrosiloxane as a selective, neutral reducing agent for aldehydes, ketones, olefins, and aromatic nitro compounds," *The Journal of Organic Chemistry*, vol. 38, no. 1, pp. 162–165, 1973.

[72] S. Hanada, Y. Motoyama, and H. Nagashima, "Dual Si-H effects in platinum-catalyzed silane reduction of carboxamides leading to a practical synthetic process of tertiary-amines involving self-encapsulation of the catalyst species into the insoluble silicone resin formed," *Tetrahedron Letters*, vol. 47, no. 35, pp. 6173–6177, 2006.